Dendritic cell-derived exosomal miR-494-3p promotes angiogenesis following myocardial infarction

HAIBO LIU[1,2*], YOUMING ZHANG[2*], JIE YUAN[3*], WEI GAO[3],
XIN ZHONG[3], KANG YAO[3], LI LIN[2] and JUNBO GE[3]

[1]Department of Cardiology, Qingpu Branch of Zhongshan Hospital, Fudan University, Shanghai 201700;
[2]Department of Cardiology, Shanghai East Hospital, Tongji University, Shanghai 200120;
[3]Shanghai Institute of Cardiovascular Diseases, Zhongshan Hospital, Fudan University, Shanghai 200032, P.R. China

Abstract. Infiltration by dendritic cells (DCs) is markedly increased in the infarcted area following myocardial infarction (MI), and DC ablation has been shown to impair angiogenesis in mice post-MI. Exosomes (EXs) have long been known to act as messengers between cells; however, whether EXs derived from DCs can enhance myocardial angiogenesis post-MI remains unknown. The aim of the present study was to elucidate whether EXs derived from DCs induce myocardial angiogenesis via paracrine signaling post-MI. *In vitro*, suspensions of mouse bone marrow-derived DCs (BMDCs) were incubated with the supernatant of necrotic or normal cultured HL-1 myocardial cells (as the MI or control group, respectively) for 24 h. EXs isolated from the supernatant of BMDCs were termed DEXs, which were added to primary cultures of rat cardiac microvascular endothelial cells (CMECs), and angiogenesis was evaluated by measuring tube formation and vascular endothelial growth factor (VEGF) expression. *In vivo*, different groups of DEXs were injected into the infarcted myocardium of MI model mice. Then, angiogenesis was evaluated by measuring the number of vessels and the expression of VEGF and CD31 in the infarcted myocardium using immunohistochemistry. Moreover, the expression profile of microRNAs (miRNAs or miRs) in splenic DCs of MI model mice was analyzed by Affymetrix miRNA 4.0 chip assays, then certified in DEXs by reverse transcription-quantitative PCR analysis. Finally, miRNA-loaded DEXs were used to induce tube formation by CMECs and angiogenesis in MI model mice. It was observed that, compared with the control group, DEXs from the MI group significantly upregulated the expression of VEGF in CMECs, enhanced tube formation by CMECs, and upregulated the expression of VEGF and CD31 in the infarcted myocardium of MI model mice. miR-494-3p and miR-16a-5p, which are associated with angiogenesis, were significantly upregulated in splenic DCs of MI model mice by Affymetrix miRNA 4.0 chip assays, miR-494-3p was significantly upregulated and highly enriched in DEXs from the MI group compared with the control, and DEX-miR-494-3p enhanced tube formation by CMECs and angiogenesis in mice post-MI. These results suggest that miR-494-3p may be secreted from DCs via EXs and promotes angiogenesis post-MI. These findings indicate a novel DEX-based approach to the treatment of MI.

Correspondence to: Dr Junbo Ge, Shanghai Institute of Cardiovascular Diseases, Zhongshan Hospital, Fudan University, 180 Fenglin Road, Shanghai 200032, P.R. China
E-mail: jbge@zs-hospital.sh.cn

Dr Li Lin, Department of Cardiology, Shanghai East Hospital, Tongji University, 150 Jimo Road, Shanghai 200120, P.R. China
E-mail: linli777@126.com

*Contributed equally

Introduction

Angiogenesis plays an important role in the recovery of the microvascular bed and prevents further apoptosis and necrosis of ischemic myocardial tissues, which may be injured, stunned or hibernating post-myocardial infarction (MI) (1). Therefore, angiogenesis is a key factor in the recovery of the ischemic myocardium and myocardial remodeling in the early stages of MI (1,2). Previous studies have demonstrated that infiltration by dendritic cells (DCs) is significantly increased in the infarcted myocardium (3-5), while angiogenesis is impaired and cardiac function is deteriorated in DC ablation mice following MI (6). These results suggest that DCs play an important role in angiogenesis and cardiac healing after MI. However, to the best of our knowledge, the mechanism underlying the effects of DCs on MI has yet to be fully elucidated.

Exosomes (EXs) are small double-membrane vesicles (30-100 nm) containing a wide range of functional proteins, mRNAs and microRNAs (miRNAs or miRs), which are secreted via exocytosis by different types of cells, including

DCs, lymphocytes and platelets, as well as cells originating from other tissues, under physiological or pathological conditions (7-9). Previous studies have demonstrated that EXs may act as mediators of cell-to-cell communication and play a key role in cardiac remodeling after MI (5,10). Furthermore, it was observed in our previous study that EXs derived from DCs (DEXs) may improve cardiac function after MI (10). However, to the best of our knowledge, whether DEXs improve cardiac function by promoting angiogenesis via paracrine signaling remains unknown.

miRNAs are short, non-coding RNAs that regulate gene expression through translational repression or degradation of target mRNAs (9). Over the last decade, miRNAs have emerged as key regulators of several cellular processes, including angiogenesis, and certain miRNAs, such as miR-132, miR-126, miR-451a, miR-494-3p, miR-16a-5p and miR-23a-3p, have been shown to play key roles in the vasculature in both endothelial and perivascular cells (11,12). In addition, previous studies have demonstrated that EXs contain a large number of miRNAs, and EXs may deliver these miRNAs to their target cells (13-15). It was previously reported that DC infiltration is significantly increased in the infarcted myocardium and plays an important role in angiogenesis and cardiac healing after MI (6). Furthermore, our previous study demonstrated that DEXs also contain abundant miRNAs that are associated with angiogenesis (16). Therefore, it may be inferred that the DCs infiltrating the infarcted myocardium may promote angiogenesis via secretion of exosomal miRNAs post-MI.

The aim of the present study was to investigate the expression and enrichment of miR-494-3p in EXs secreted from DCs post-MI, and determine whether it can promote angiogenesis *in vitro* and *in vivo*.

Materials and methods

Study design. An outline of the design of the present study is shown in Fig. 1. In brief, C57BL/6 mice served as donors for the culture of bone marrow-derived DCs (BMDCs) and as MI models. Then, samples were collected from the supernatants of necrotic HL-1 cells, which were incubated with BMDCs for 24 h as the MI group. Samples from the supernatants of normal cells served as the control group, and from the culture medium of BMDCs as the negative group. Subsequently, DEXs from different groups were isolated and added to primary cultures of rat cardiac microvascular endothelial cells (CMECs), confocal microscopy was performed to observe the interaction of CMECs with DEXs, and angiogenesis was evaluated through measuring tube formation and vascular endothelial growth factor (VEGF) expression. For the *in vivo* experiments, DEXs from different groups were injected into the infarcted myocardium of MI model mice, and angiogenesis was evaluated by measuring the expression of VEGF and CD31 in the infarcted myocardium and the mean number of CD31-positive capillaries were counted in the infarcted area under an optical microscope. Finally, the expression profile of miRNAs in splenic DCs of MI model mice was analyzed by Affymetrix miRNA 4.0 chip assays, and those miRNAs associated with angiogenesis that were significantly upregulated in the Affymetrix miRNA 4.0 chip were also certified in DCs and DEXs by reverse transcription-quantitative PCR (RT-qPCR)

analysis. Subsequently, it was evaluated whether the significantly upregulated and highly enriched DEX-miR-494-3p could enhance tube formation *in vitro* and angiogenesis *in vivo*.

Animals. Male, wild-type mice (C57BL/6) and newborn male Sprague-Dawley rats were purchased from the Shanghai Laboratory Animal Center. Male, 6-week-old C57BL/6 mice (weight, 16-20 g; n=30) were used for culture of BMDCs and the newborn rats (age, 1-2 days; weight, 5-6 g; n=20) were used for culture of CMECs. In addition, 8-week-old male C57BL/6 mice (weight, 22-28 g, n=30) were used to construct the MI models and were subjected to DEX injections. All the mice and rats were housed under pathogen-free conditions in a standard laboratory with a controlled room temperature (22±1˚C) and humidity (65-70%), and a 12:12-h light-dark cycle, with free access to food and water. Animal care and treatment complied with the standards approved by the Institutional Review Board of Zhongshan Hospital of Fudan University and the Shanghai Institutes of Biological Sciences-CAS (A5894-01).

Culture of BMDCs and CMECs. BMDCs were isolated from C57BL/6 mice. BMDCs were cultured with a non-serum medium (X-VIVO 15; Lonza Group, Ltd.) to eliminate the interference of exosomes from FBS, as described previously (17). Briefly, the mice were sacrificed by cervical dislocation and the femurs were isolated. The bone marrow cells were washed out from the femurs and cultured in non-serum medium containing 10 ng/ml granulocyte-macrophage colony-stimulating factor and 1 ng/ml IL-4 (both from R&D Systems, Inc.). The medium was changed every other day. On day 7, the BMDCs were collected and treated as previously described (17). CMECs were isolated from newborn rats. Briefly, the rats were sacrificed by cervical dislocation and immersed in 75% ethanol for 10 min. Then, the hearts were excised and rinsed with 4˚C Hank's Balanced Salt Solution (HyClone; Cytiva), followed by resecting the left ventricular tissue and removing the epicardium and endocardium. The remaining tissues were cut into 1-mm^3 pieces and inoculated into 10-cm culture dishes with 1 ml FBS (Gibco; Thermo Fisher Scientific, Inc.). The tissues were then cultured in a 37˚C, 5% CO_2 incubator for 4 h, and for a further 72 h in high-glucose DMEM (Invitrogen; Thermo Fisher Scientific, Inc.) supplemented with 20% FBS. When the endothelial cells reached a confluence of 90%, the tissues were removed carefully and digested with 0.125% trypsin (Gibco; Thermo Fisher Scientific, Inc.). The cells were transferred to another culture dish and the second generation of cells were used for subsequent experiments. All the experiments were performed under sterile conditions.

Simulation of post-MI cardiomyocyte microenvironment in vitro. Three types of samples were used to mimic the MI microenvironment: i) The supernatants of necrotic HL-1 cells; ii) the supernatants of hypoxic primary cardiomyocytes; and iii) the supernatants of infarcted mouse myocardium, which have been described in detail in our previous study (10). The results of the previous study suggested that treatment with the supernatants of necrotic HL-1 cells or hypoxic primary cardiomyocytes *in vitro* activates DCs in mice to a similar extent as MI. In the present study, the supernatants of necrotic HL-1 cells were used to mimic the MI microenvironment. In
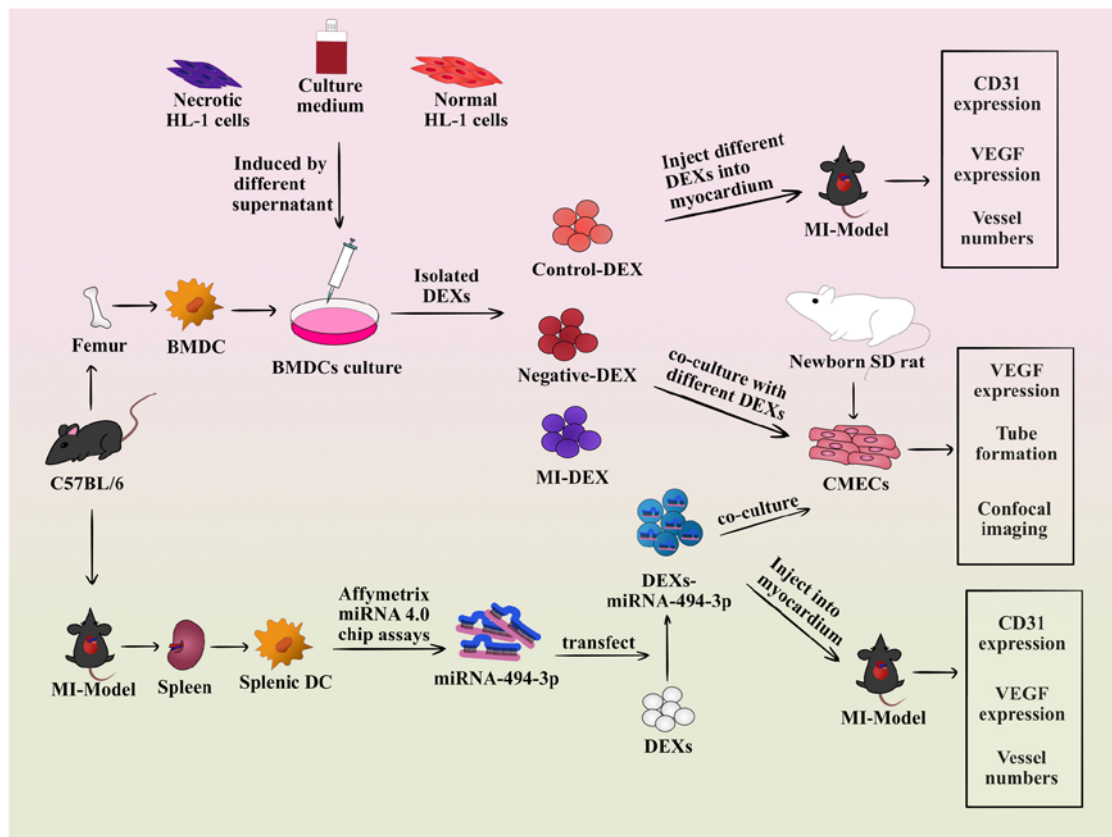
Figure 1. Flowchart of the design of the present study. In brief, C57BL/6 mice served as donors for the culture of BMDCs and as MI models. Samples were collected from the supernatants of necrotic HL-1 cells, which were incubated with BMDCs for 24 h as the MI group. Samples from the supernatants of normal cells served as the control group, and samples from the culture medium of BMDCs served as the negative group. Subsequently, DEXs from different groups were isolated and added to primary cultures of rat CMECs, followed by angiogenesis evaluation through measuring tube formation and VEGF expression. Confocal microscopy was performed to observe the interaction of CMECs with DEXs. For the *in vivo* experiments, DEXs from different groups were injected into the infarcted myocardium of MI model mice, and angiogenesis was evaluated by measuring the expressions of VEGF and CD31 in the infarcted myocardium and the mean number of vessel counts in the infarcted area. Finally, the expression profile of miRNAs in splenic DCs of MI model mice was analyzed by Affymetrix miRNA 4.0 chip assays, and those miRNAs associated with angiogenesis that were significantly upregulated in the Affymetrix miRNA 4.0 chip were also certified in DCs and DEXs by reverse transcription-quantitative PCR analysis. Subsequently, it was evaluated whether the significantly upregulated and highly enriched miR-494-3p could enhance tube formation *in vitro* and angiogenesis *in vivo*. DEXs, dendritic cell-derived exosomes; BMDC, bone marrow-derived dendritic cell; MI, myocardial infarction; DC, dendritic cell; SD, Sprague-Dawley; miRNA-494-3p, microRNA-494-3p; CMECs, cardiac microvascular endothelial cells; VEGF, vascular endothelial growth factor.

brief, 100-μl samples, from which the cell membrane particles were removed by centrifugation at 1,500 x g at room temperature for 30 min, were collected from the supernatants of the necrotic HL-1 cells (MI group) and added to 1x10^6 BMDCs for 24 h. The same conditions were used with the supernatant from normal cells (control group) or 100 μl of culture medium from the culture of DCs (negative group). All the experiments were performed under sterile conditions.

DEX isolation. The ExoQuick-TC™ Exosome Precipitation Solution (System Biosciences Inc.) was used to isolate DEXs, according to the protocol recommended by the manufacturer. Briefly, 1/5 volume of ExoQuick-TC™ Exosome Precipitation Solution was added to 10 ml supernatant of DCs and refrigerated overnight at 4˚C. Then, the samples were centrifuged at 1,500 x g at room temperature for 30 min and the supernatant was removed. The DEXs were re-suspended in 1 ml PBS (HyClone; Cytiva). DEXs were divided into 3 groups as follows: i) MI DEX group: DEXs isolated from BMDCs stimulated by the supernatant of necrotic HL-1 cells; ii) control DEX group: DEXs isolated from BMDCs stimulated by the supernatant

of normal HL-1 cells; and iii) negative DEX group: DEXs isolated by adding the same amount of BMDC medium. The details were described in our previous study (10).

Interaction of CMECs with DEXs by confocal laser scanning microscopy. DEXs were labeled with PKH67 at room temperature for 10 min (green; Sigma-Aldrich; Merck KGaA) and co-cultured with CMECs, and confocal laser scanning microscopy was used to observe the interaction between CMECs and DEXs. Briefly, 25,000 CMECs were co-cultured with 100 μl PKH67-labeled DEXs for 24 h. Then, the supernatant was discarded, followed by washing twice with PBS, fixation for 10 min at room temperature with 4% paraformaldehyde (Sangon Biotech Co., Ltd.) and staining for 15 min at room temperature with phalloidin-TRITC (Thermo Fisher Scientific, Inc.) and DAPI (Invitrogen; Thermo Fisher Scientific, Inc.). Subsequently, the cells were observed using a confocal laser scanning microscope (magnification, x630; Leica TCS SP8; Leica Microsystems GmbH; 40x or 60x/1.30 NA HCX PL APO CS OIL objective lens) and images were captured using the Leica application suite Advanced Fluorescence Lite

and analyzed using LAS AF Lite V4.3.1 software (National Institutes of Health).

Tube formation assay. Matrigel™ basement membrane matrix (growth factor reduced) (BD Biosciences) was thawed at 4°C overnight, and then transferred into precooled 24-well plates and incubated at 37°C for 30 min. Subsequently, CMECs, which had been divided into four groups [unstimulated group, negative DEX group (addition of negative DEXs, 100 μl), control DEX group (addition of control DEXs, 100 μl) and MI DEX group (addition of MI DEXs, 100 μl)], were seeded onto the 24 well-plates (25,000 cells per well, three wells per group), then cultured in a 37°C, 5% CO_2 incubator with 1% FBS-DMEM. Finally, images were captured at 3, 6, 9, 12 and 24 h using the BH-2 inverted optical microscope (magnification, x50; Olympus Corporation) for the enclosed networks of complete tubes. The tube formation images were analyzed by the WimTube Image Analysis V 7.02 software (Ibidi GmbH).

Detection of VEGF expression in CMECs in vitro. After co-culturing negative, control and MI DEXs with CMECs for 24 h, the expression of VEGF in CMECs was detected by western blotting. Briefly, CMECs were collected and lysed in RIPA lysis buffer (Sigma-Aldrich; Merck KGaA) containing 1% protease inhibitors (cOmplete Protease Inhibitor Cocktail; Roche Diagnostic, Inc.). Following centrifugation at 14,000 x g for 20 min at 4°C and discarding the sediment, the lysates were loaded in SDS buffer containing 50 mM DTT (Invitrogen; Thermo Fisher Scientific, Inc.) and heated at 100°C for 5 min. Then, proteins (10 μg/lane) were separated by 12% SDS-PAGE (Sigma-Aldrich; Merck KGaA) and transferred to PVDF membranes (EMD Millipore). After blocking with 5% BSA (Sigma-Aldrich; Merck KGaA) for 2 h at room temperature, the membranes were incubated with mouse anti-VEGF monoclonal antibody (Abcam; cat. no. ab69479; 1:500) or mouse anti-GAPDH (Abcam; cat. no. ab8245; 1:1,000) overnight at 4°C. After the membranes were washed with TBST (Sigma-Aldrich; Merck KGaA) three times, they were incubated with goat anti-mouse IgG horseradish peroxidase-conjugated secondary monoclonal antibody (Abcam; cat. no. ab205719; 1:2,000) at room temperature for 2 h, followed by washing in TBST. Finally, the membranes were exposed using the LAS-3000 imager system (Fujifilm Corporation), and the image analysis and the densitometric analysis to semi-quantify the protein expression data were performed using Quantity One V 4.6.6 software (Bio-Rad Laboratories, Inc.).

MI model induction and injection of DEXs. Coronary artery ligation was used to induce the MI model (18). Briefly, mice were anaesthetized by 2% isoflurane inhalation (RWD Life Science) with an isoflurane delivery system (Harvard Bioscience, Inc.). A small incision was made on the skin of the left chest, followed by dissecting and retracting the major and minor pectoral muscles. Next, a clamp was used to create a small hole in the 4th intercostal space and open the pleural membrane. The clamp was then opened slightly and the heart was extracted. The left coronary artery (LCA) was ligated with a 6-0 silk suture and the heart was immediately placed back into the intrathoracic cavity. Finally, the air was evacuated and the skin was sutured. Mice undergoing the same surgical procedure, but without LCA ligation, were used as the sham group. After successfully constructing the MI model, 10 μg negative, control or MI DEXs were injected into the left ventricle in five sites around the infarct area, as described previously (19).

Detection of the expression of VEGF and CD31 in the infarcted myocardium. On day 7, MI model mice were sacrificed by cervical dislocation and the expression of VEGF and CD31 was determined by immunohistochemistry, as previously described (19). Briefly, tissue sections from heart samples were fixed with 4% paraformaldehyde at room temperature for 24-48 h. Then, paraffin-embedded murine heart samples were cut into 5-μm-thick tissue sections, and dewaxed in xylene (Sangon Biotech Co., Ltd.) and rehydrated using ethanol. Then, antigen retrieval was performed with boiling 0.01 M citrate buffer (Sangon Biotech Co., Ltd.) and, after using 3% hydrogen peroxide (Sangon Biotech Co., Ltd.) to eliminate the endogenous peroxidase activity, the sections were incubated with goat serum blocking solution (Abcam) for 15 min at room temperature. Next, the sections were incubated overnight at 4°C with anti-CD31 (Abcam; cat. no. ab9498; 1:2,000) and anti-VEGF (Abcam; cat. no. ab1316; 1:200). After washing three times with PBS, sections were incubated with horseradish peroxidase-labeled goat anti-rabbit IgG (Abcam; cat. no. ab5879; 1:500) for 15 min at 37°C. After DAB color reaction (using the DAB Horseradish Peroxidase Color Development Kit; Sangon Biotech Co., Ltd.) and hematoxylin (Sangon Biotech Co., Ltd.) counterstaining for 1 min at room temperature, the sections were sealed with neutral gum and observed under an optical microscope (magnification, x400; Olympus Corporation).

miRNA expression profile in splenic DCs of MI mice. At 24 h and on day 7, MI model mice were sacrificed by cervical dislocation and the spleens were removed and crushed to prepare the splenic single-cell suspension. Subsequently, the method of positive selection was used with anti-CD11c$^+$ microbeads (Miltenyi Biotec GmbH) according to the manufacturers' instructions to obtain purified CD11c$^+$ DCs. Next, TRIzol® reagent (Invitrogen; Thermo Fisher Scientific, Inc.) was used to extract total RNA from DCs, according to the manufacturers' instructions. Finally, the total RNA was sent to Beijing Boao Biological Co., Ltd. for quality testing, and Affymetrix miRNA 4.0 microarray for miRNAs screening was performed after passing the quality testing.

Detection of miRNA expression within DEXs. miRcute miRNA extraction and isolation kit (Tiangen Biochemical Technology Co., Ltd.) was used to extract miRNA in DEXs following the manufacturer's instructions. Then, the miRcute miRNA First-Strand cDNA Synthesis Kit (Tiangen) was used to generate cDNA from miRNA according to the manufacturer's instructions. The miRcute miRNA qPCR Detection Kit (SYBR Green; Tiangen) was used for qPCR following the manufacturer's instructions. The reactions were incubated in a 96-well plate at 94°C for 2 min, followed by 40 cycles of 94°C for 20 sec and 60°C for 34 sec on an Applied Biosystems 7500 Real-time PCR System (Thermo Fisher Scientific, Inc.).
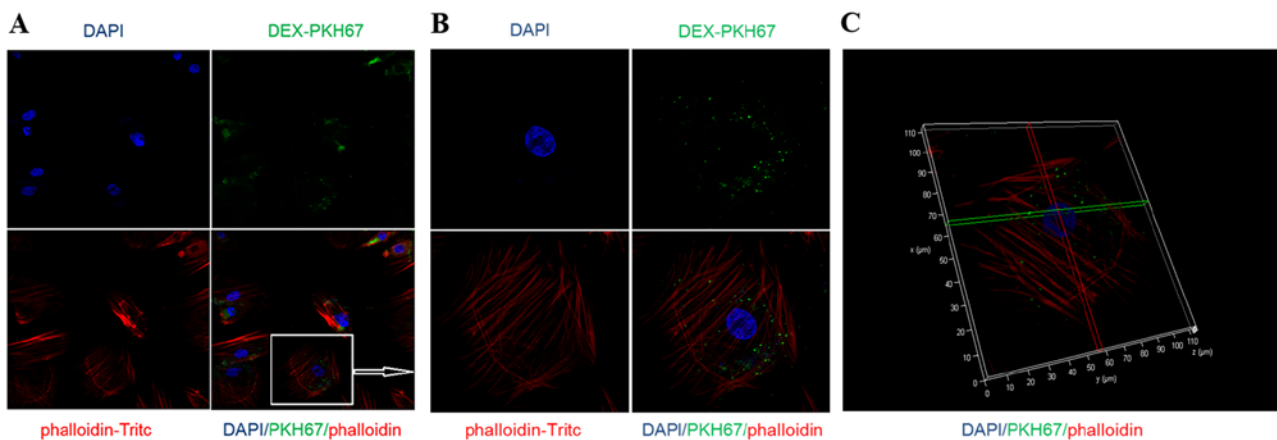
Figure 2. Interaction of CMECs with DEXs by confocal imaging. (A) DEXs uptake by CMECs; (B) enlarged image of (A). (C) 3D imaging of a single cell: The cell nucleus is stained with DAPI (blue), cell microfilaments are stained with phalloidin (red), and DEXs are stained with PKH67 (green). Magnification, x630. CMECs, cardiac microvascular endothelial cells; DEX, dendritic cell-derived exosome.

To calculate the relative fold change values, the Cq values were normalized to U6 miRNA as internal control. Analysis was performed using the $2^{-\Delta\Delta Cq}$ method (20). Primers were synthesized by Tiangen Biochemical Technology Co., Ltd. (Hsa-miR-494-3p; stock no. MIMAT0002816; Hsa-U6; stock no. CD201-0145). The mature sequence of miR-494-3p was 5'-UGAAACAUACACGGGAAACCUC-3'.

miR-494-3p transfection into DEXs. miR-494-3p mimic, inhibitor and their scrambled negative controls were purchased from Qiagen (cat. nos. 219600, 219300, 1027281 and 1027271, respectively) and transfected into normal cultured BMDCs *in vitro*. Briefly, BMDCs were plated in 6-well plates and cultured overnight. Then, the BMDCs were transfected with 10 nM miR-494-3p mimic, 50 nM inhibitor or 10 nM scrambled sequence using riboFECTTM CP Reagent (Guangzhou RiboBio Co., Ltd.) according to the manufacturer's protocol. Successful transfection was confirmed by RT-qPCR assessment of the expression of miR-494-3p. BMDCs only treated with riboFECTTM CP Reagent without miRNAs were considered as the blank group and those transfected with the scrambled negative controls were used as the negative control (NC) group. Following transfection, BMDCs were cultured with a non-serum medium (X-VIVO 15; Lonza Group, Ltd.) in a 37˚C, 5% CO_2 incubator for 24 h. Then, DEXs were isolated as described above. Finally, DEXs were co-cultured with CMECs and tube formation assay was performed, or DEX-miR-494-3p were injected into the infarcted myocardium in MI model mice, as described above.

Statistical analysis. All results presented are from at least three independent experiments for each condition. Data are expressed as the mean ± standard deviation. Statistical analysis was performed using GraphPad Prism 5 software (GraphPad Prism Software Inc.). Differences among groups were examined using either One-way ANOVA (parametric method) or Kruskal-Wallis test (non-parametric method) according to the results of normality and homogeneity tests of variance. If there was a statistically significant difference among groups, a post hoc test was applied to evaluate the difference between groups. In this case, Bonferroni's test was used for parametric data and Dunn's test was used for non-parametric data. $P<0.05$ was considered to indicate a statistically significant difference.

Results

DEXs are taken up by CMECs. After co-culturing PKH67-labeled DEXs with CMECs, confocal laser scanning microscopy was used to examine whether DEXs were taken up by CMECs, and it was observed that CMECs were able to directly take up DEXs (Fig. 2).

Effects of DEXs on CMECs. After determining, using confocal laser scanning microscopy, that DEXs could be taken up by CMECs, the effects of DEXs on CMECs were examined. Matrigel was used to perform a tube formation assay with CMECs and explore the effects of negative, control and MI DEXs on tube formation by CMECs. It was observed that MI DEXs, compared with negative and control DEXs, significantly promoted the tube formation ability of CMECs at 6 h ($P<0.05$; Fig. 3A and B). After co-culturing negative, control and MI DEXs with CMECs for 24 h, the expression of VEGF in CMECs was detected by western blotting. It was observed that MI DEXs significantly upregulated VEGF expression in CMECs compared with negative, negative DEXs and control DEXs (Fig. 3C and D).

MI DEXs promote angiogenesis in mice after MI. After the *in vitro* experiments demonstrated that DEXs affected CMECs, the effects of DEXs on the myocardium *in vivo* were investigated. The immunohistochemistry results revealed that the expression of CD31 and VEGF in the infarcted myocardium of MI model mice was markedly increased in the MI DEXs compared with the MI, negative DEXs and control DEXs (Fig. 4A). Furthermore, the mean number of vessels in the infarcted myocardium was significantly increased in the MI DEX compared with non-injected, negative DEXs and control DEXs (Fig. 4B). These results suggested that injection of MI DEXs promoted angiogenesis after MI in mice.

miRNA expression in DCs from mice after MI. Our previous experiments demonstrated that DEXs could enhance
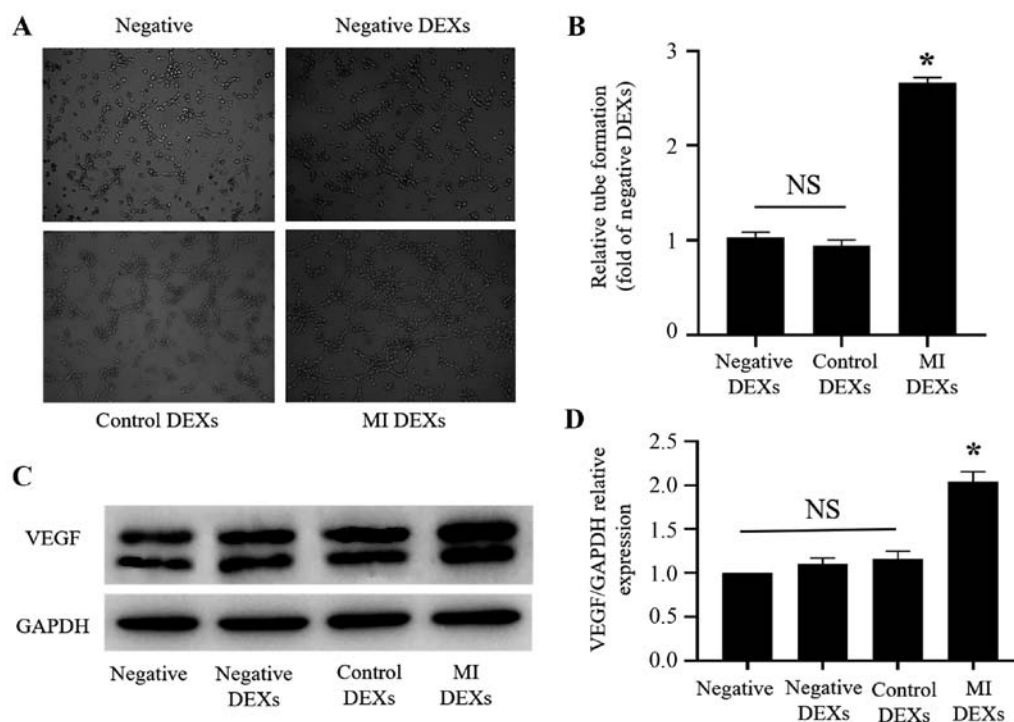
Figure 3. MI DEXs enhance tube formation by CMECs at 6 h. (A) Induction of tube formation by CMECs by different groups of DEXs. Magnification, x50. (B) Statistical results of (A) (n=5). *P<0.05 vs. negative DEXs and control DEXs. (C) The expression of VEGF in CMECs induced by DEXs as determined by western blotting. (D) The densitometric analysis to semi-quantify the protein expression data from the western blots from (C) *P<0.05 vs. negative, negative DEXs and control DEXs (n=3). GAPDH was used to normalize the data. MI, myocardial infarction; CMECs, cardiac microvascular endothelial cells; DEXs, dendritic cell-derived exosomes; VEGF, vascular endothelial growth factor; NS, not significant.
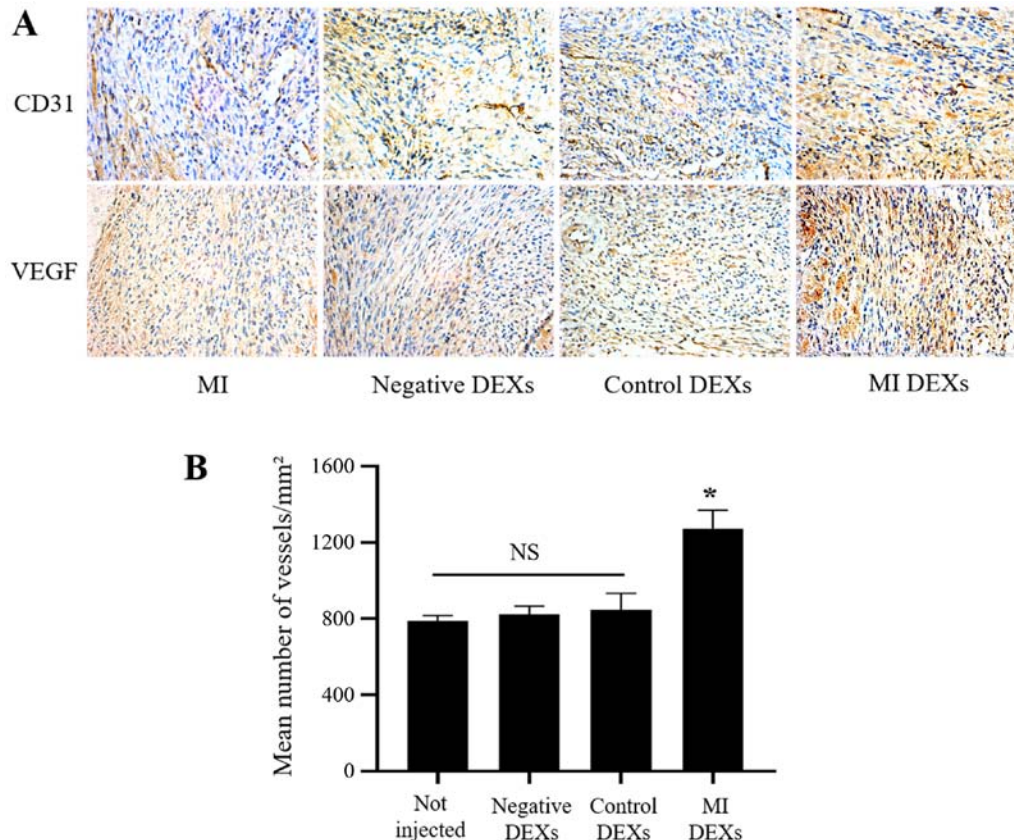

Figure 4. DEXs induce angiogenesis in MI model mice. (A) The expression of CD31 and VEGF was determined by immunohistochemistry in the infarcted myocardium of MI model mice. Magnification, x400. (B) Comparison of vessel counts in the infarcted area among different groups (n=6-7). *P<0.05 vs. not injected, negative DEXs and control DEXs. NS, not significant; MI, myocardial infarction; DEXs, dendritic cell-derived exosomes; VEGF, vascular endothelial growth factor.
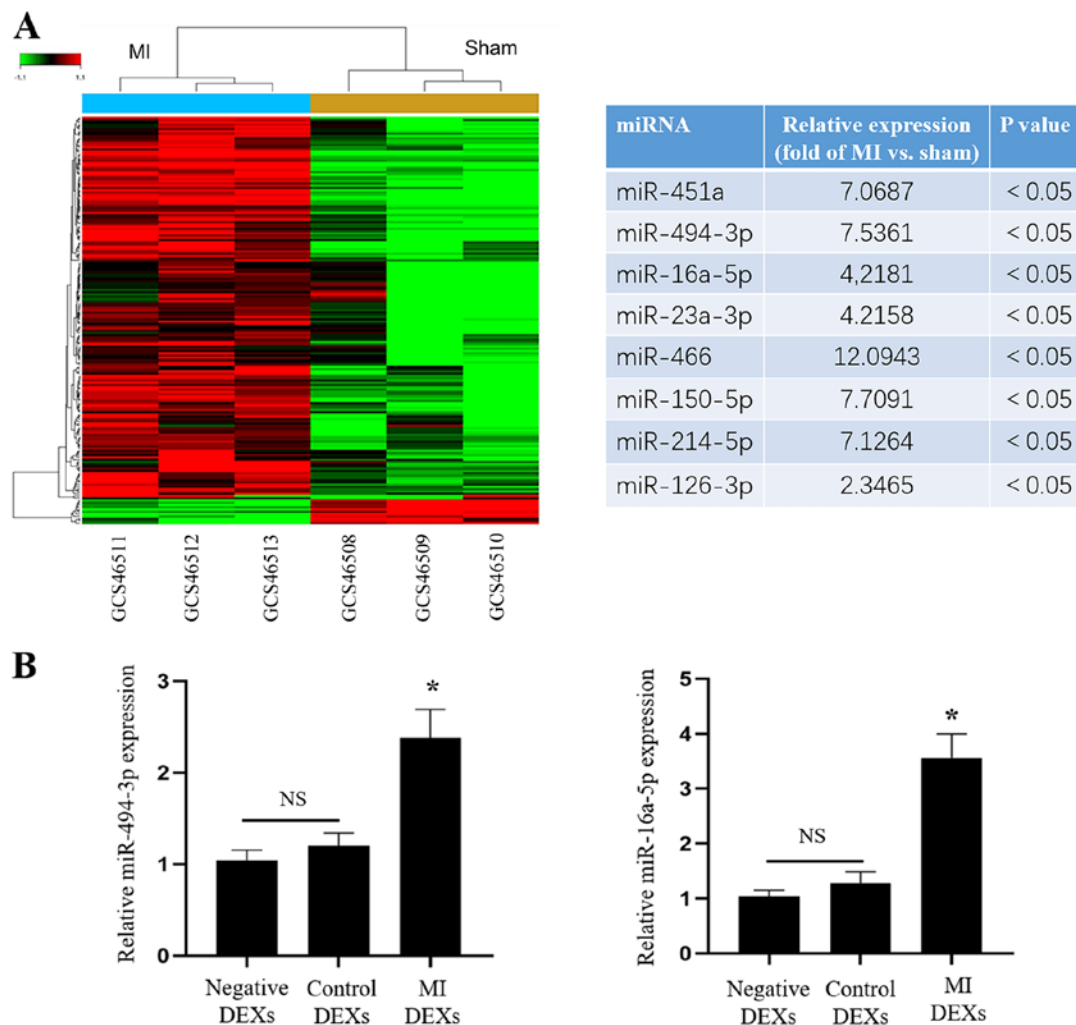
miRNA	Relative expression (fold of MI vs. sham)	P value
miR-451a	7.0687	< 0.05
miR-494-3p	7.5361	< 0.05
miR-16a-5p	4,2181	< 0.05
miR-23a-3p	4.2158	< 0.05
miR-466	12.0943	< 0.05
miR-150-5p	7.7091	< 0.05
miR-214-5p	7.1264	< 0.05
miR-126-3p	2.3465	< 0.05

Figure 5. Gene chip screening of miRNAs certified by RT-qPCR analysis. (A) Gene chip screening of miRNAs in mouse splenic DCs by Affymetrix miRNA 4.0 microarrays. (B) The expression levels of miR-494-3p and miR-16a-5p were determined by RT-qPCR in different groups. *P<0.05 vs. negative DEXs and control DEXs (n=3). NS, not significant; MI, myocardial infarction; DCs, dendritic cells; DEXs, dendritic cell-derived exosomes; RT-qPCR, reverse transcription-quantitative PCR; miRNA or miR, microRNA.

angiogenesis *in vitro* as well as *in vivo*, but the mechanisms through which DEXs exert their effects remained unknown. A large number of studies have shown that EXs contain various miRNAs, some of which are associated with angiogenesis. Therefore, gene chip screening for the expression of miRNAs in splenic DCs of MI model mice was performed, and revealed that the expression levels of miR-451a, miR-494-3p, miR-16a-5p miR-23a-3p, miR-466, miR-150-5p, miR-214-5p and miR-126-3p which are associated with angiogenesis, were significantly increased compared with that in sham mice (P<0.05; Fig. 5A). Then, RT-qPCR was used to detect the expression of angiogenesis-related miRNAs, and the expression of miR-494-3p and miR-16a-5p was also found to be significantly increased in MI DEXs compared with that in negative DEXs and control DEXs (P<0.05; Fig. 5B), but other miRNAs were not significantly increased. The enhancement of tube formation by miR-16a-5p *in vitro* was not observed in our previous experiments, therefore miR-494-3p was selected for further experiments in the present study.

DEX-miR-494-3p enhances tube formation in CMECs in vitro. miR-494-3p mimic and inhibitor were transfected into BMDCs,

and successful transfection was confirmed by RT-qPCR analysis of miR-494-3p expression, which was significantly increased in the mimic and significantly reduced in the inhibitor compared with the blank and NC (Fig. 6A and B). It was observed that DEX-miR-494-3p mimic significantly enhanced the tube formation by CMECs at 6 h (P<0.05; Fig. 6C and D), while DEX-miR-494-3p inhibitor significantly inhibited tube formation by CMECs compared with DEXs-blank and DEXs-NC (P<0.05; Fig. 6E and F).

DEX-miR-494-3p promotes angiogenesis after MI in mice. Our previous experiments revealed that DEX-miR-494-3p enhanced tube formation by CMECs *in vitro*. It was next investigated whether DEX-miR-494-3p mimic induced angiogenesis *in vivo*. DEXs injected into the infarcted myocardium in MI model mice were used, and it was observed that DEX-miR-494-3p mimic markedly increased the expression of CD31 and VEGF in the infarcted myocardium, while DEX-miR-494-3p inhibitor markedly decreased CD31 and VEGF expression compared with the DEXs blank and DEXs NC (Fig. 7A and C). In addition, the mean number of vessels in the infarcted myocardium was significantly increased in the
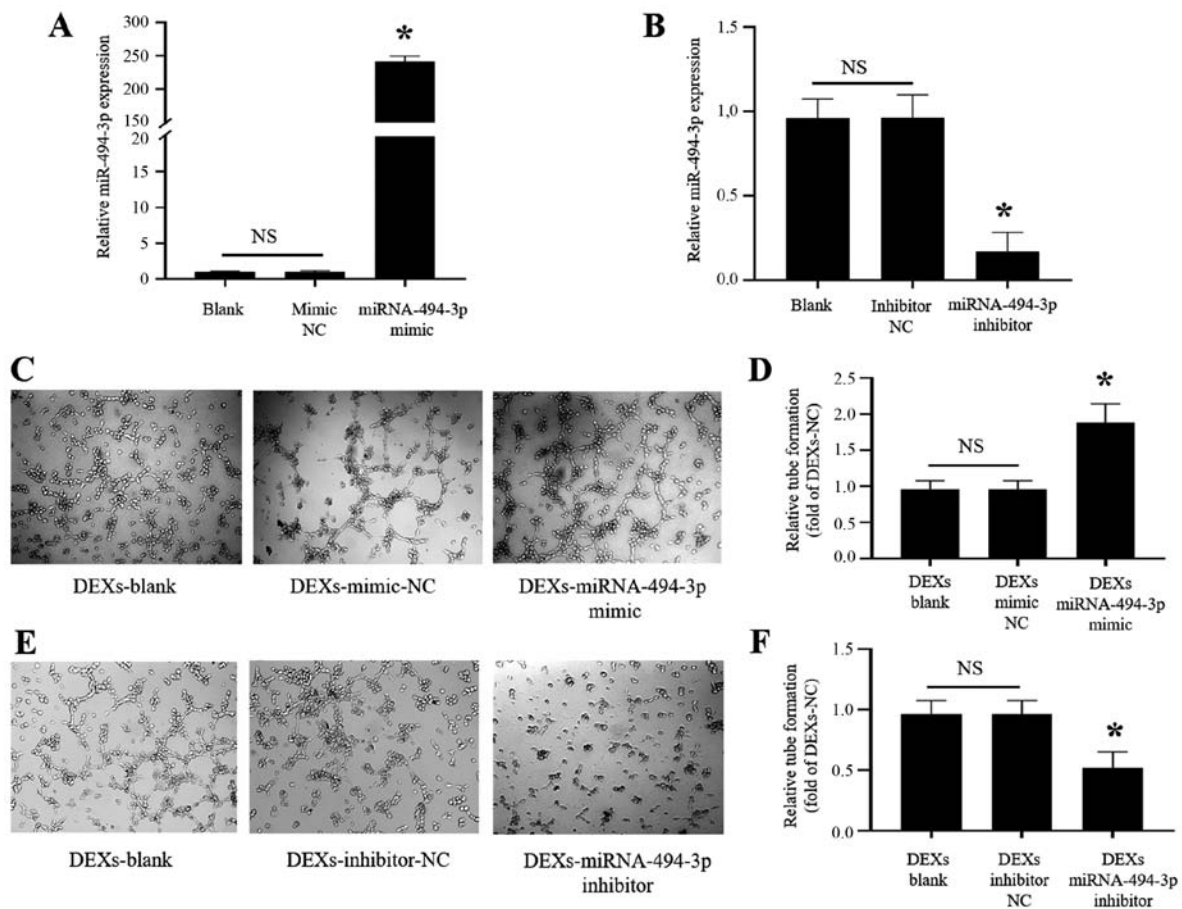
Figure 6. DEXs-miR-494-3p enhances tube formation by CMECs. (A) The expression level of miR-494-3p in BMDCs was determined by RT-qPCR following transfection with miR-494-3p mimic. *P<0.05 vs. blank and mimic NC. (B) The expression level of miR-494-3p in BMDCs was determined by RT-qPCR following transfection with miR-494-3p inhibitor. *P<0.05 vs. blank and inhibitor NC. (C) Tube formation by CMECs transfected with miR-494-3p mimic at 6 h was observed under an inverted optical microscope. Magnification, x50. (D) Statistical results of (C) *P<0.05 vs. DEXs blank and DEXs mimic NC. (E) Tube formation by CMECs transfected with miR-494-3p inhibitor at 6 h was observed under an inverted optical microscope. Magnification, x50. (F) Statistical results of (E). *P<0.05 vs. DEXs blank and DEXs inhibitor NC. NS, not significant; CMECs, cardiac microvascular endothelial cells; DEXs, dendritic cell-derived exosomes; miRNA or miR, microRNA; NC, negative control; RT-qPCR, reverse transcription-quantitative PCR.

DEX-miR-494-3p mimic group and significantly decreased in the DEX-miR-494-3p inhibitor group compared with the DEXs blank and DEXs NC groups (Fig. 7B and D).

Discussion

In the present study, it was demonstrated that EXs secreted by DCs can be directly taken up by CMECs. Furthermore, MI DEXs significantly upregulated VEGF expression in CMECs and enhanced tube formation and angiogenesis in the infarcted myocardium of MI model mice. Gene chip screening and RT-qPCR validation revealed that the expressions of miR-494-3p and miR-16a-5p, which are associated with angiogenesis, were significantly increased in MI DEXs, and further studies revealed that transfer of miR-494-3p mimic into DEXs significantly enhanced tube formation by CMECs and angiogenesis in the infarcted myocardium of MI model mice.

Our previous study demonstrated that MI DEXs could significantly improve cardiac function in mice after MI (10). The present study demonstrated that MI DEXs could increase the number of vessels and the expression of CD31 and VEGF in the infarcted myocardium, which indicated that EXs

derived from DCs may improve cardiac function by inducing myocardial angiogenesis via paracrine signaling post-MI.

A large number of studies have demonstrated that EXs are the mediators of cell-to-cell communication. EXs secreted from cells can directly act on or be taken up by other cells and play a role in regulating the function of target cells (21-23). Previous studies have also reported that EXs play an important role in myocardial healing and cardiac remodeling after MI (8,17,21,24). Khan *et al* (21) observed that EXs extracted from embryonic stem cells could promote the repair of injured myocardial tissue and improve cardiac function and survival rate of mice after MI. Teng *et al* (25) demonstrated that bone marrow mesenchymal stem cell-derived EXs enhanced angiogenic capacity and significantly improved cardiac function after MI in rats. However, the majority of previous studies focused on the role of EXs secreted by stem cells, cardiomyocytes or fibroblasts (21,26), while to the best of our knowledge, there is still no relevant report on the role of EXs secreted by immune inflammatory cells in the repair of myocardial injury after MI.

It has been demonstrated that immune inflammatory cells, including DCs, play a key role in cardiac remodeling and are implicated in cardiac angiogenesis after MI (6,27,28);
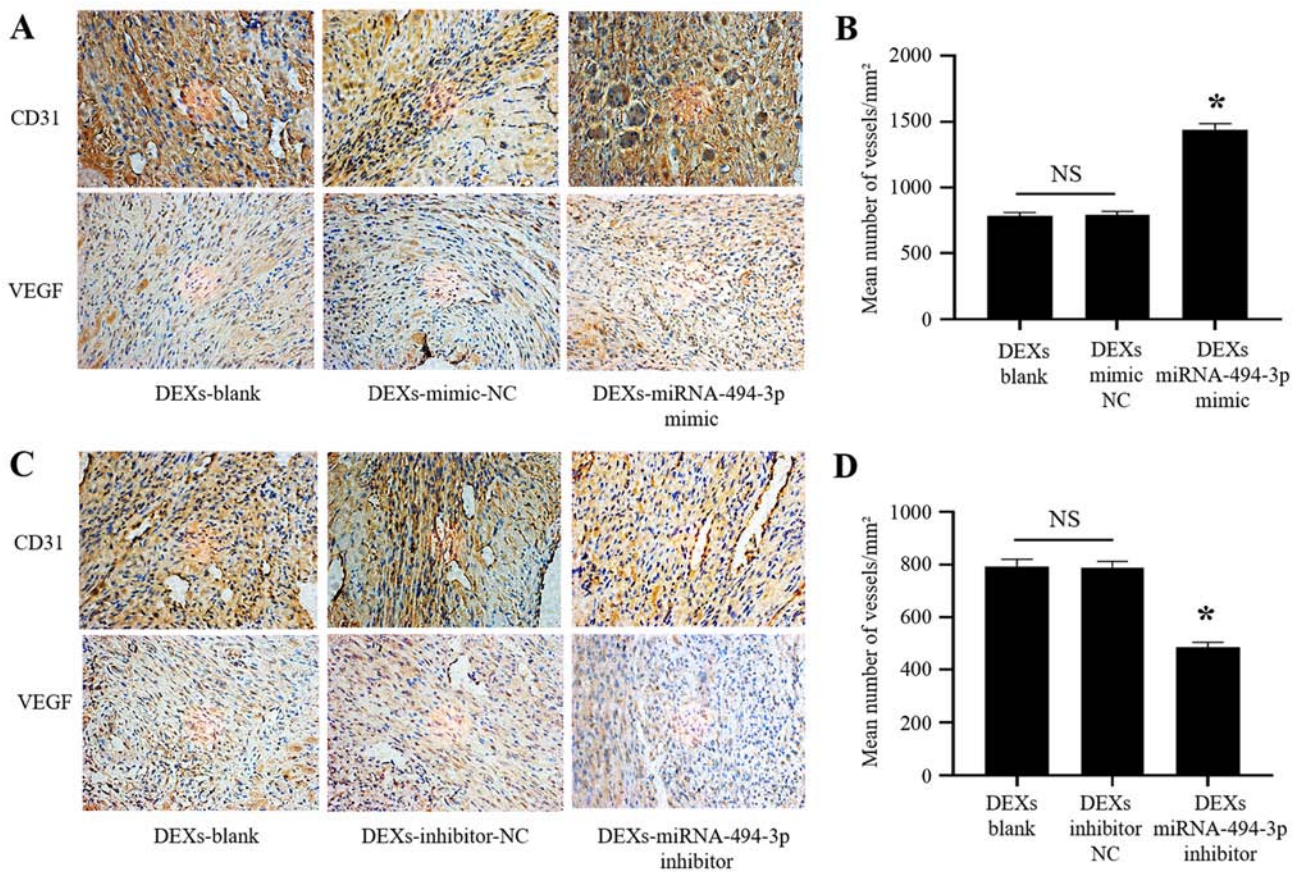
Figure 7. DEXs-miRNA-494-3p induces angiogenesis in MI model mice. (A) The expression levels of CD31 and VEGF in the infarcted myocardium of MI model mice induced by DEXs-miRNA-494-3p mimic were determined by immunohistochemistry. (B) Comparison of vessel counts in the infarcted area among different groups (n=6-7). *P<0.05 vs. DEXs blank and DEXs mimic NC. (C) The expression of CD31 and VEGF in the infarcted myocardium of MI model mice induced by DEXs-miRNA-494-3p inhibitor was determined by immunohistochemistry. (D) The mean number of CD31-positive capillaries/mm² were counted in the infarcted area in five fields per sample under an optical microscope and compared among different groups (n=6-7). *P<0.05 vs. DEXs blank and DEXs inhibitor NC. Magnification, x400. NS, not significant; MI, myocardial infarction; DEXs, dendritic cell-derived exosomes; VEGF, vascular endothelial growth factor; miRNA, microRNA; NC, negative control.

however, whether DCs promote angiogenesis by secreting DEXs remains unknown, to the best of our knowledge. The present study demonstrated that MI DEXs significantly upregulated the expression of VEGF in CMECs and enhanced tube formation and angiogenesis in the infarcted myocardium of MI model mice, which indicated that the DCs infiltrating the infarcted myocardium post-MI may promote angiogenesis by secreting DEXs, and the angiogenesis following MI plays an important role in the recovery of the injured myocardium and maintenance of cardiac function (29).

Regarding the mechanism through which DEXs promote angiogenesis post-MI, previous studies demonstrated that EXs secreted by cells contain a large number of miRNAs (21,26), some of which have been confirmed by several studies to be associated with angiogenesis (11,12,30,31). Therefore, the miRNAs in splenic DCs of MI model mice were screened using Affymetrix miRNA 4.0 microarrays, and the expression levels of miR-451a, miR-494-3p and miR-16a-5p, which are associated with angiogenesis, were found to be significantly increased compared with that in sham mice. Then, these miRNAs were examined in MI DEXs by RT-qPCR and the expression of miR-494-3p and miR-16a-5p was also found to be significantly increased in MI DEXs. miR-494-3p was then transferred into DEXs, and DEX-miR-494-3p was used

to induce tube formation by CMECs and angiogenesis in MI model mice. The results demonstrated that DEX-miR-494-3p significantly enhanced tube formation by CMECs and angiogenesis in MI model mice post-MI, which indicated that the effect of DEXs on myocardium is partially mediated by the high expression of miRNAs within DEXs.

Previous studies have reported the association between miR-494 and angiogenesis, but the conclusions have been inconsistent. Mao et al (32) found that tumor-derived miR-494 could promote angiogenesis in cell carcinoma. However, Welten et al observed that inhibition of miRNA clusters in the 14q32 region, including miR-494, increased angiogenesis as well as recanalization after peripheral vascular ischemia (33). In the present study, miR-494-3p significantly enhanced tube formation by CMECs in vitro and angiogenesis in MI model mice. Thus, the role of miR-494 in angiogenesis is not entirely consistent across different disease models and requires further in-depth investigation.

In conclusion, the present study demonstrated that DCs can promote angiogenesis by secreting DEXs after MI, which is partially achieved by delivery of highly expressed miRNAs in DEXs. These findings indicate a novel DEX-miRNA-based approach to MI treatment. There are some limitations in the present study; it did not identify the target of miR-494-3p and

how this affects the angiogenic pathways post-MI and the cell signaling events downstream. Therefore, the underlying molecular mechanisms require further elucidation by future studies.

Availability of data and materials

The datasets used and/or analyzed during the current study are available from the corresponding author on reasonable request.

Authors' contributions

HL performed the cell culture, exosome isolation and tube formation assay. YZ determined microRNA expression by reverse transcription-quantitative PCR analysis. JY performed cell transfection. HL, YZ and JY wrote the manuscript. WG and XZ constructed the myocardial infarction mouse model and performed the injection of DEXs. KY performed confocal laser scanning microscopy examination. LL discussed the results, commented on the manuscript and analyzed the data. JG designed the experiments and analyzed the data. All authors read and approved the final manuscript.

Ethics approval and consent to participate

The present study was approved by the Institutional Review Board of Zhongshan Hospital of Fudan University and the Shanghai Institutes of Biological Sciences-CAS (approval no. A5894-01).

Patient consent for publication

Not applicable.

Competing interests

The authors declare that they have no competing interests.

References

1. van der Laan AM, Piek JJ and van Royen N: Targeting angiogenesis to restore the microcirculation after reperfused MI. Nat Rev Cardiol 6: 515-523, 2009.
2. Shah AM and Mann DL: In search of new therapeutic targets and strategies for heart failure: Recent advances in basic science. Lancet 378: 704-712, 2011.
3. Frangogiannis NG: Regulation of the inflammatory response in cardiac repair. Circ Res 110: 159-173, 2012.
4. Yan X, Anzai A, Katsumata Y, Matsuhashi T, Ito K, Endo J, Yamamoto T, Takeshima A, Shinmura K, Shen W, *et al*: Temporal dynamics of cardiac immune cell accumulation following acute myocardial infarction. J Mol Cell Cardiol 62: 24-35, 2013.
5. Montecalvo A, Larregina AT, Shufesky WJ, Stolz DB, Sullivan ML, Karlsson JM, Baty CJ, Gibson GA, Erdos G, Wang Z, *et al*: Mechanism of transfer of functional microRNAs between mouse dendritic cells via exosomes. Blood 119: 756-766, 2012.
6. Anzai A, Anzai T, Nagai S, Maekawa Y, Naito K, Kaneko H, Sugano Y, Takahashi T, Abe H, Mochizuki S, *et al*: Regulatory role of dendritic cells in postinfarction healing and left ventricular remodeling. Circulation 125: 1234-1245, 2012.
7. Zhang D, Lee H, Zhu Z, Minhas JK and Jin Y: Enrichment of selective miRNAs in exosomes and delivery of exosomal miRNAs in vitro and in vivo. Am J Physiol Lung Cell Mol Physiol 312: L110-L121, 2017.
8. Emanueli C, Shearn AIU, Angelini GD and Sahoo S: Exosomes and exosomal miRNAs in cardiovascular protection and repair. Vascul Pharmacol 71: 24-30, 2015.
9. Vlassov AV, Magdaleno S, Setterquist R and Conrad R: Exosomes: Current knowledge of their composition, biological functions, and diagnostic and therapeutic potentials. Biochim Biophys Acta 1820: 940-948, 2012.
10. Liu H, Gao W, Yuan J, Wu C, Yao K, Zhang L, Ma L, Zhu J, Zou Y and Ge J: Exosomes derived from dendritic cells improve cardiac function via activation of CD4$^+$ T lymphocytes after myocardial infarction. J Mol Cell Cardiol 91: 123-133, 2016.
11. Tiwari A, Mukherjee B and Dixit M: MicroRNA key to angiogenesis regulation: MiRNA biology and therapy. Curr Cancer Drug Targets 18: 266-277, 2018.
12. Sun P, Zhang K, Hassan SH, Zhang X, Tang X, Pu H, Stetler RA, Chen J and Yin KJ: Endothelium-targeted deletion of microRNA-15a/16-1 promotes post-stroke angiogenesis and improves long-term neurological recovery. Circ Res 126: 1040-1057, 2020.
13. Lin Y, Zhang C, Xiang P, Shen J, Sun W and Yu H: Exosomes derived from HeLa cells break down vascular integrity by triggering endoplasmic reticulum stress in endothelial cells. J Extracell Vesicles 9: 1722385, 2020.
14. Liu S, Chen J, Shi J, Zhou W, Wang L, Fang W, Zhong Y, Chen X, Chen Y, Sabri A and Liu S: M1-like macrophage-derived exosomes suppress angiogenesis and exacerbate cardiac dysfunction in a myocardial infarction microenvironment. Basic Res Cardiol 115: 22, 2020.
15. Kang JY, Park H, Kim H, Mun D, Park H, Yun N and Joung B: Human peripheral bl004derived exosomes for microRNA delivery. Int J Mol Med 43: 2319-2328, 2019.
16. Liu H, Yuan J, Gao W, Wu C, Yao K, Zhang L, Guo X, Yu W, Zou Y and Ge J: Exosomes secreted from dendritic cells enhance tube formation in cardiac microvascular endothelial cells after myocardial infarction. In: European Heart Journal 36: Suppl 1: 1958, 2015.
17. Alexander M, Hu R, Runtsch MC, Kagele DA, Mosbruger TL, Tolmachova T, Seabra MC, Round JL, Ward DM and O'Connell RM: Exosome-delivered microRNAs modulate the inflammatory response to endotoxin. Nat Commun 6: 7321, 2015.
18. Gao E, Lei YH, Shang X, Huang ZM, Zuo L, Boucher M, Fan Q, Chuprun JK, Ma XL and Koch WJ: A novel and efficient model of coronary artery ligation and myocardial infarction in the mouse. Circ Res 107: 1445-1453, 2010.
19. Huang K, Liu J, Zhang H, Wang J and Li H: Intramyocardial injection of siRNAs can efficiently establish myocardial tissue-specific renalase knockdown mouse model. Biomed Res Int 2016: 1267570, 2016.
20. Livak KJ and Schmittgen TD: Analysis of relative gene expression data using real-time quantitative PCR and the 2(-Delta Delta C(T)) method. Methods 25: 402-408, 2001.

21. Khan M, Nickoloff E, Abramova T, Johnson J, Verma SK, Krishnamurthy P, Mackie AR, Vaughan E, Garikipati VN, Benedict C, *et al*: Embryonic stem cell-derived exosomes promote endogenous repair mechanisms and enhance cardiac function following myocardial infarction. Circ Res 117: 52-64, 2015.

22. Bang C, Batkai S, Dangwal S, Gupta SK, Foinquinos A, Holzmann A, Just A, Remke J, Zimmer K, Zeug A, *et al*: Cardiac fibroblast-derived microRNA passenger strand-enriched exosomes mediate cardiomyocyte hypertrophy. J Clin Invest 124: 2136-2146, 2014.

23. Sun X, He S, Wara AK, Icli B, Shvartz E, Tesmenitsky Y, Belkin N, Li D, Blackwell TS, Sukhova GK, *et al*: Systemic delivery of microRNA-181b inhibits nuclear factor-κB activation, vascular inflammation, and atherosclerosis in apolipoprotein E-deficient mice. Circ Res 114: 32-40, 2014.

24. Xiao X, Lu Z, Lin V, May A, Shaw DH, Wang Z, Che B, Tran K, Du H and Shaw PX: MicroRNA miR-24-3p reduces apoptosis and regulates Keap1-Nrf2 pathway in mouse cardiomyocytes responding to ischemia/reperfusion injury. Oxid Med Cell Longev 2018: 7042105, 2018.

25. Teng X, Chen L, Chen W, Yang J, Yang Z and Shen Z: Mesenchymal stem cell-derived exosomes improve the microenvironment of infarcted myocardium contributing to angiogenesis and anti-inflammation. Cell Physiol Biochem 37: 2415-2424, 2015.

26. Gao W, Liu H, Yuan J, Wu C, Huang D, Ma Y, Zhu J, Ma L, Guo J, Shi H, *et al*: Exosomes derived from mature dendritic cells increase endothelial inflammation and atherosclerosis via membrane TNF-α mediated NF-κB pathway. J Cell Mol Med 20: 2318-2327, 2016.

27. Hofmann U and Frantz S: Role of T-cells in myocardial infarction. Eur Heart J 37: 873-879, 2016.

28. Hofmann U and Frantz S: Role of lymphocytes in myocardial injury, healing, and remodeling after myocardial infarction. Circ Res 116: 354-367, 2015.

29. Nishida M, Carley WW, Gerritsen ME, Ellingsen O, Kelly RA and Smith TW: Isolation and characterization of human and rat cardiac microvascular endothelial cells. Am J Physiol 264: H639-H652, 1993.

30. Zeng Z, Li Y, Pan Y, Lan X, Song F, Sun J, Zhou K, Liu X, Ren X, Wang F, *et al*: Cancer-derived exosomal miR-25-3p promotes pre-metastatic niche formation by inducing vascular permeability and angiogenesis. Nat Commun 9: 5395, 2018.

31. Sun Z, Shi K, Yang S, Liu J, Zhou Q, Wang G, Song J, Li Z, Zhang Z and Yuan W: Effect of exosomal miRNA on cancer biology and clinical applications. Mol Cancer 17: 147, 2018.

32. Mao G, Liu Y, Fang X, Liu Y, Fang L, Lin L, Liu X and Wang N: Tumor-derived microRNA-494 promotes angiogenesis in non-small cell lung cancer. Angiogenesis 18: 373-382, 2015.

33. Welten SM, Bastiaansen AJ, De Jong RC, de Vries MR, Peters EA, Boonstra MC, Sheikh SP, Monica NL, Kandimalla ER, Quax PH and Nossent AY: Inhibition of 14q32 MicroRNAs miR-329, miR-487b, miR-494, and miR-495 increases neovascularization and blood flow recovery after ischemia. Circ Res 115: 696-708, 2014.